# Supplementary materials

## Antibacterial Activities and Life Cycle Stages of *Asparagopsis armata*: Implications of the Metabolome and Microbiome

Christelle Parchemin*[,1,2], Delphine Raviglione[1], Anouar Mejait[1], Pierre Sasal[1], Elisabeth Faliex[2], Camille Clerissi[1], Nathalie Tapissier-Bontemps[1]

[1] **C**entre de **R**echerches **I**nsulaires et **Ob**servatoire de l'**E**nvironnement (CRIOBE), UAR 3278 UPVD-EPHE-CNRS, Université de Perpignan - Via Domitia, 52 Av. Paul Alduy, 66860 Perpignan CEDEX, France

[2] **CE**ntre de **F**ormation et de **R**echerche sur les **E**nvironnements **M**éditerranéens (CEFREM), UMR 5110 UPVD-CNRS, Université de Perpignan - Via Domitia, 52 Av. Paul Alduy, 66860 Perpignan CEDEX, France

*Corresponding authors: Christelle Parchemin (christelle.parchemin@univ-perp.fr); Nathalie Tapissier-Bontemps (nathalie.tapissier@univ-perp.fr)

# Table of contents

Supplementary methods ..... 4

Supplementary method 1: Pictures of the stages of *A. armata* life cycle collected in Banyuls-sur-Mer with the tetrasporophyte (A), the gametophyte without cystocarps (B) and the gametophyte with developed cystocarps (C) ..... 4

Supplementary method 2: Details of data pre-processing for the metabolomics study ..... 4

Supplementary method 3: Composition of bacterial media. The quantities (in g) correspond to the preparation of 1 L of medium ..... 5

Supplementary figures ..... 6

Figure S1: Hierarchical clustering analysis of the metabolome of three stages of the life cycle of *A. armata* analysed in UHPLC-ESI(-)-HRMS/MS (distance measure: Euclidean, clustering algorithm: Ward) ..... 6

Figure S2: Chromatogram of a quality control sample analysed with the UHPLC-ESI(-)-HRMS spectrometer and displaying the ion at *m/z* 572.50134 $[M-H]^-$ (most intense isotopic mass) of the molecule $C_5H_2Br_6O_2$ with the highest intensity on the chromatogram. ..... 7

Figure S3: Chromatogram of the most active fractions (flash-chromatography fractionation) analysed by UHPLC-ESI(-)-HRMS/MS ..... 8

Figure S4: ESI(-)-MS/MS spectrum of $C_5H_2Br_6O_2$ (compound 1) and the possible fragmentation pattern. ..... 9

Figure S5: ESI(-)-MS/MS spectrum of $C_5H_2Br_5ClO_2$ (compound 2) and the possible fragmentation pattern. ..... 9

Figure S6: ESI(-)-MS/MS spectrum of $C_5H_3Br_4ClO_2$ (compound 5) and the possible fragmentation pattern. ..... 10

Figure S7: ESI(-)-MS/MS spectrum of $C_4H_3Br_3O_3$ (compound 6) and the possible fragmentation pattern. ..... 10

Figure S8: ESI(-)-MS/MS spectrum of $C_5H_3Br_5O_2$ (compound 7) and the possible fragmentation pattern. ..... 11

Figure S9: Chromatogram of the most active fractions of the second fractionation (HPLC (Waters 1525) coupled to a UV detector (Waters 2487)) analysed by UHPLC-ESI(-)-HRMS/MS ..... 12

Figure S10: EIC of ion with a *m/z* 572.5021 (most abundant isotopic mass) corresponding to a monoisotopic m/z of 566.5085 in active fractions, including 40 % $H_2O$-MeOH (A), 30 % $H_2O$-MeOH (B), F9 (C) and F10 (D)..... 13

Figure S11: Rarefaction curves of 16S rRNA gene sequences for the gametophyte with developed cystocarps (A), the gametophyte (B) and the tetrasporophyte (C) samples. ..... 14

Figure S12: Relative abundance of bacterial families associated with the three *A. armata* stages. Codes "C" represents samples of the gametophyte with developed cystocarps, "G" the gametophyte samples and "T" the tetrasporophyte samples. ..... 15

Figure S13: KO pathways of the most predicted abundant functions associated with GC (A), G (B) and T (C)..... 16

Figure S14: Scores plot of the multiblock PLS-DA analysis (DIABLO) of *A. armata* gametophyte *(G)*, with developed cystocarps *(GC)*, and tetrasporophyte *(T)* phases. ..... 17

Figure S15: Correlations between the first dimension (A) and the second dimension (B) of each dataset (Chem= Chemistry; Metabarc= Metabarcoding) for the two PLS models. Codes "C" represents samples of the gametophyte with developed cystocarps, "G" the gametophyte samples and "T" the tetrasporophyte samples. ..... 18

Figure S16: Heatmap of significant ASV and metabolites of the three phases of *A. armata* ("C" represents samples of the gametophyte with developed cystocarps, "G" the gametophyte samples and "T" the tetrasporophyte samples)..... 19

# Supplementary methods

**Supplementary method 1: Pictures of the stages of *A. armata* life cycle collected in Banyuls-sur-Mer with the tetrasporophyte (A), the gametophyte without cystocarps (B) and the gametophyte with developed cystocarps (C)**

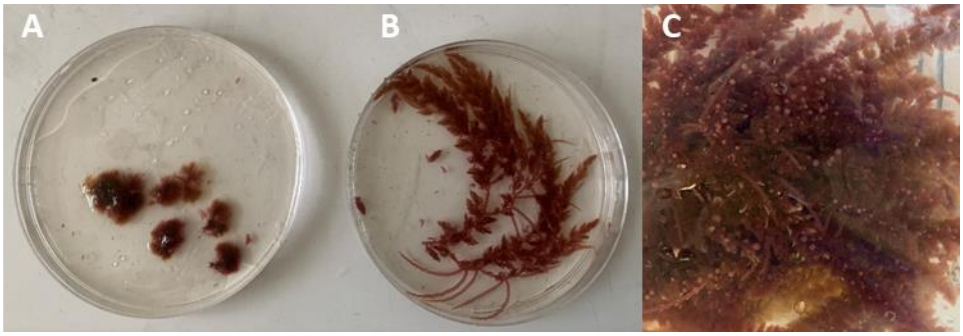


**Supplementary method 2: Details of data pre-processing for the metabolomics study**

Data acquisitions were performed using Xcalibur 4.1.31.9 (Thermo Fisher Scientific). Raw data were converted to mzML files with MSconvert (version 3.0, from Proteowizard library). mzML files were uploaded and processed using the Galaxy web platform (version 3.3) (Giacomoni et al., 2015; Guitton et al., 2017). The workflow used for data pre-processing and used parameters are published on the Galaxy Workflow4Metabolomics platform at: https://workflow4metabolomics.usegalaxy.fr/u/christelle_parchemin/w/workflowparcheminalgae. Briefly, the preprocessing consisted in a chromatographic peak detection (Galaxy Version 3.12+galaxy0) using the CentWave method with a minimum and maximum peak width of 5 and 60s, and 4 successive scans with an intensity above 500 000 as limit for consideration of region of interest. The chromotagraphic peak detection was followed by a peak grouping using the PeakDensity method step, a loess/non-linear "PeakGroups" retention time adjustment (degree of smoothing: 0.8), a peak filling and "CAMERA" peak annotation. A matrix of features with peak intensity, m/z value and retention time was generated. A clean-up based on p-Values and t-Stat outputs generated by the "CAMERA" step was performed in order to eliminate all features that are significantly detected in blanks. Then, an "inter/intra-batch" signal correction was applied using the "Batch correction" function with a "loess" regression model (span = 0.8) (Van Der Kloet et al., 2009). This step was followed by a second clean-up according to feature's CV in pool QC injections (all features with area relative standard deviation upper than 30% through pool QC injections were eliminated from the

dataset) (Thévenot et al., 2015). Finally, redundancies due to isotopes were manually eliminated (only monoisotopic mass was kept). For identification, most probable molecular formula was determined using using Sirius (v4.9.15 (Dührkop et al., 2019))), MetLin database, characteristics isotopic clusters, MS/MS spectra and comparison with literature.

## Supplementary method 3: Composition of bacterial media. The quantities (in g) correspond to the preparation of 1 L of medium

| Code | Strain | Medium | Culture temperature (°C) | Incubation time (h) | Susceptible to antibiotic |
|---|---|---|---|---|---|
| *Ea* | *Edwardsiella anguillarum* (DSMZ-27202) | Luria Broth[a] | 27 | 24 | Kanamycine |
| *Lg* | *Lactococcus garvieae* (CIP102507T) | Brain Heart Infusion[b] | 37 | 24 | Erythromycine |
| *Tm* | *Tenacibaculum martimum* (CIP103528T) | Marine Broth[c] | 27 | 24 | Ampicilline |
| *Va* | *Vibrio anquillarum* (CIP 63.36T) | Marine Broth[c] | 27 | 24 | Kanamycine |
| *Vh* | *Vibrio harveyi* (CIP103192T) | Marine Broth[c] | 27 | 24 | Kanamycine |
| *Yr* | *Yersina ruckeri* (CIP82.80T) | Marine Broth[c] | 27 | 24 | Amoxicilline |

[a]Luria Broth = 5 g of yeast extract (Yeast Extract 70161-500G (Fluka Analytical, Sigma-Aldrich®, Saint-Louis USA)), 10g of peptone (Peptone from casein, pancreatic digest 70169-500G (Fluka Analytical, Sigma-Aldrich®, Saint-Louis USA)), 10g of sea salts (Sea salts S9883-500G (Sigma Life Science, Sigma-Aldrich®, Saint-Louis USA)) and 15 g of bacteriological agar (Bacteriological agar A5306-250G (Sigma-Aldrich®, Saint-Louis USA)).
[b]Brain Heart Infusion Agar = 52 g for 1 L of medium (Brain Heart Infusion Agar 70138-500G (Sigma-Aldrich®, Saint-Louis USA))
[c]Marine Broth = 37.4 g for 1 L of medium (Difco™ Marine Broth 2216 (Becton, Dickinson and Company, Sparks, USA))

# Supplementary figures

**Figure S1: Hierarchical clustering analysis of the metabolome of three stages of the life cycle of *A. armata* analysed in UHPLC-ESI(−)-HRMS/MS (distance measure: Euclidean, clustering algorithm: Ward)**

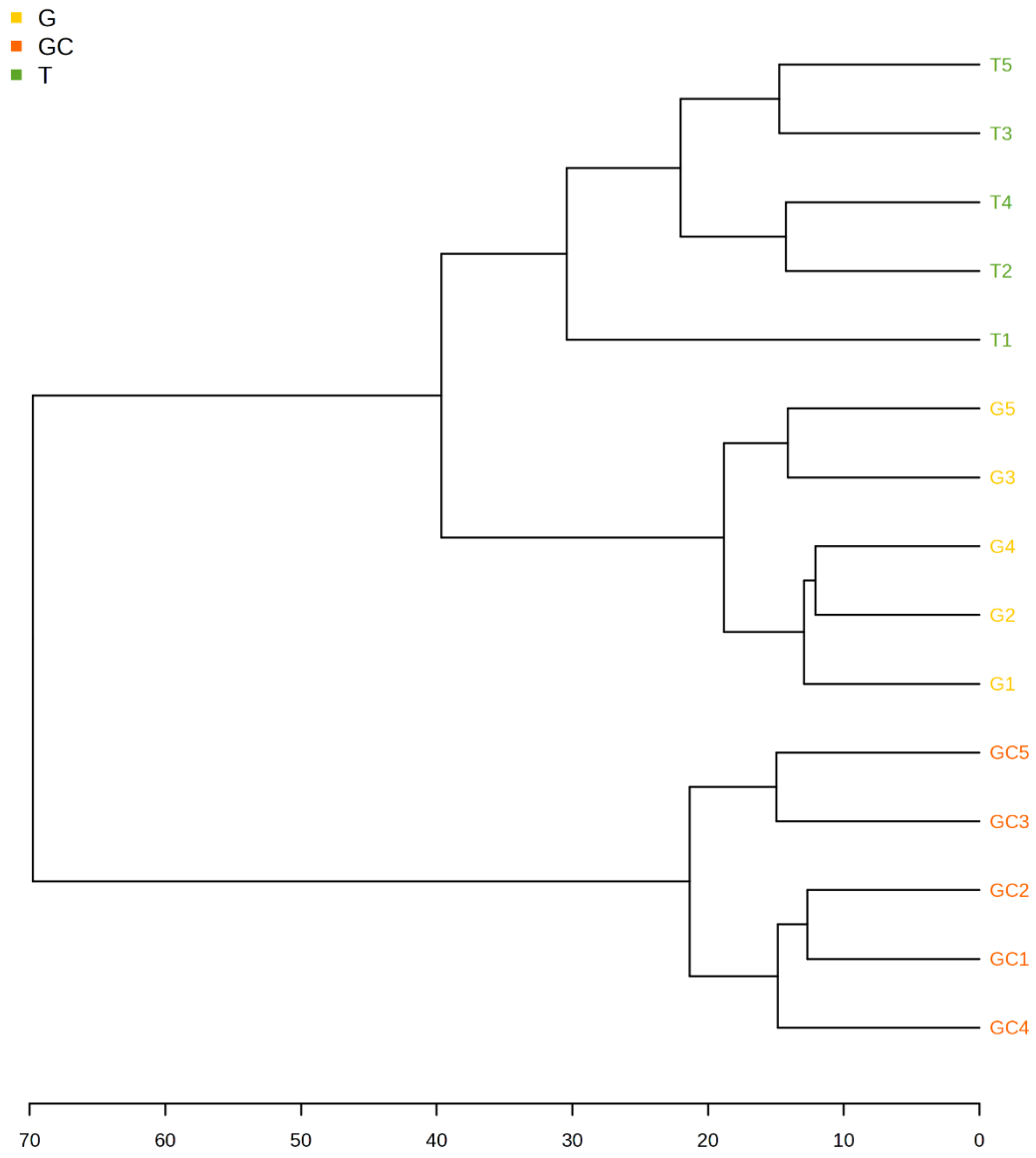

**Figure S2: Chromatogram of a quality control sample analysed with the UHPLC-ESI(−)-HRMS spectrometer and displaying the ion at *m/z* 572.50134 $[M-H]^-$ (most intense isotopic mass) of the molecule $C_5H_2Br_6O_2$ with the highest intensity on the chromatogram.**

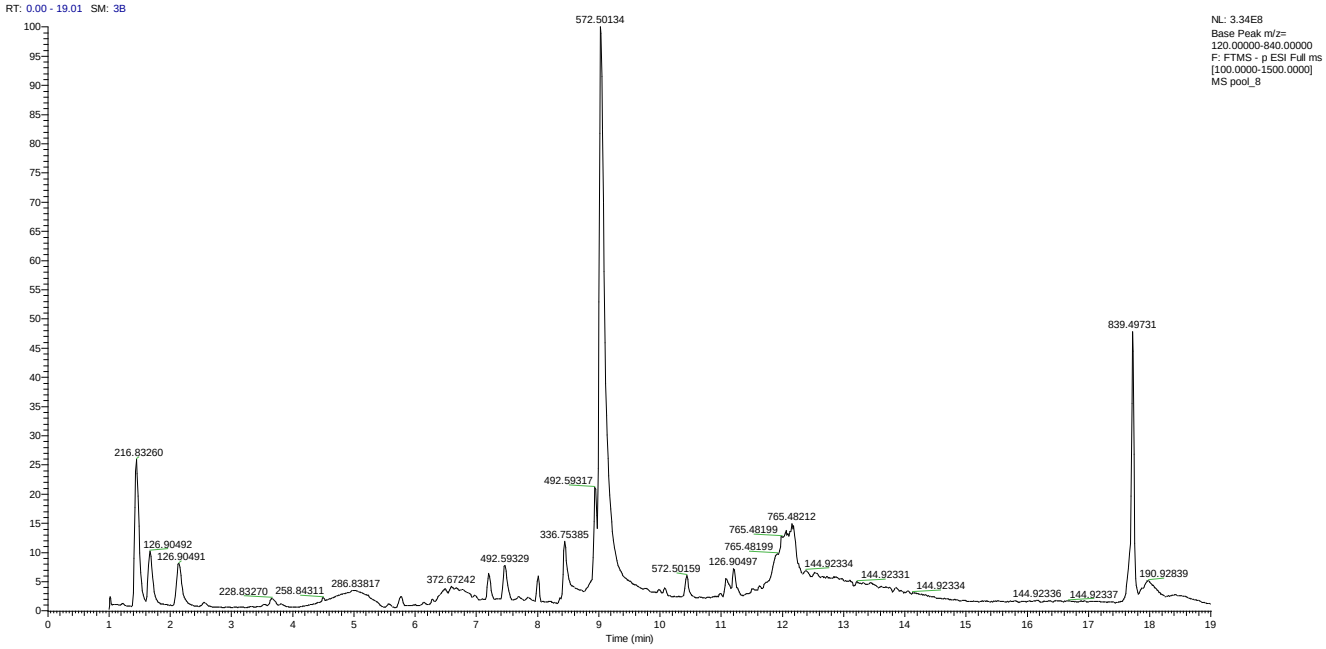

**Figure S3: Chromatogram of the most active fractions (flash-chromatography fractionation) analysed by UHPLC-ESI(−)-HRMS/MS**

A. 40 % $H_2O$-MeOH (98.9±0.4 % of bacterial growth inhibition)

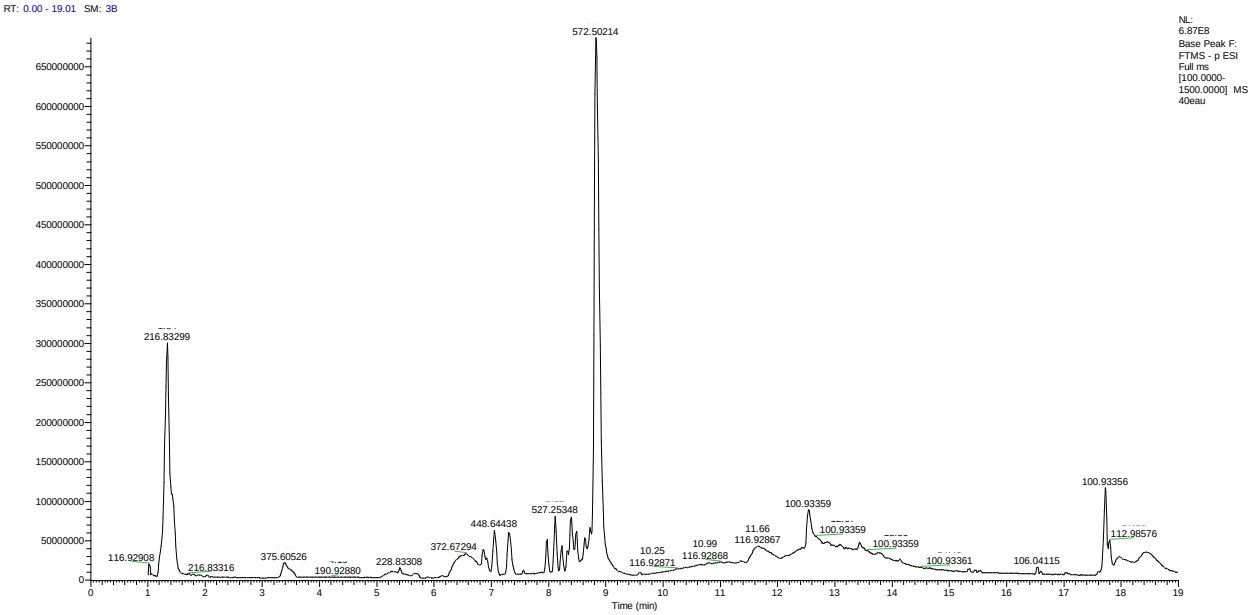


B. 30 % $H_2O$-MeOH (97.6±0.8 % of bacterial growth inhibition)

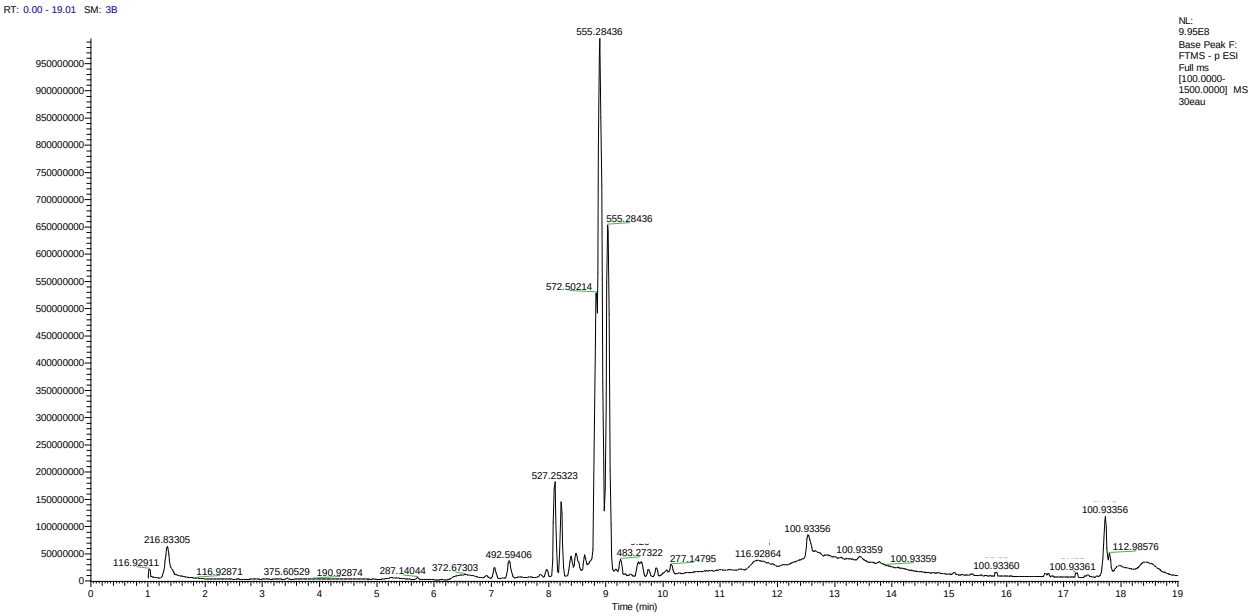

**Figure S4: ESI(−)-MS/MS spectrum of $C_5H_2Br_6O_2$ (compound 1) and the possible fragmentation pattern.**

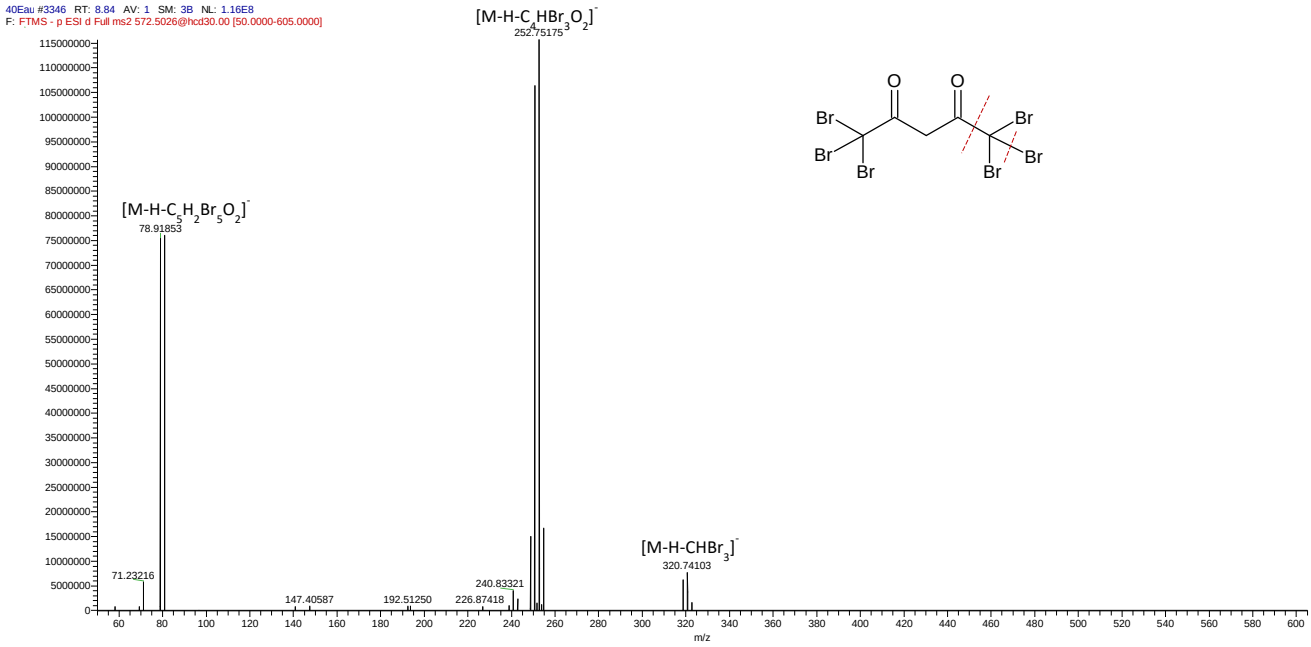


**Figure S5: ESI(−)-MS/MS spectrum of $C_5H_2Br_5ClO_2$ (compound 2) and the possible fragmentation pattern.**

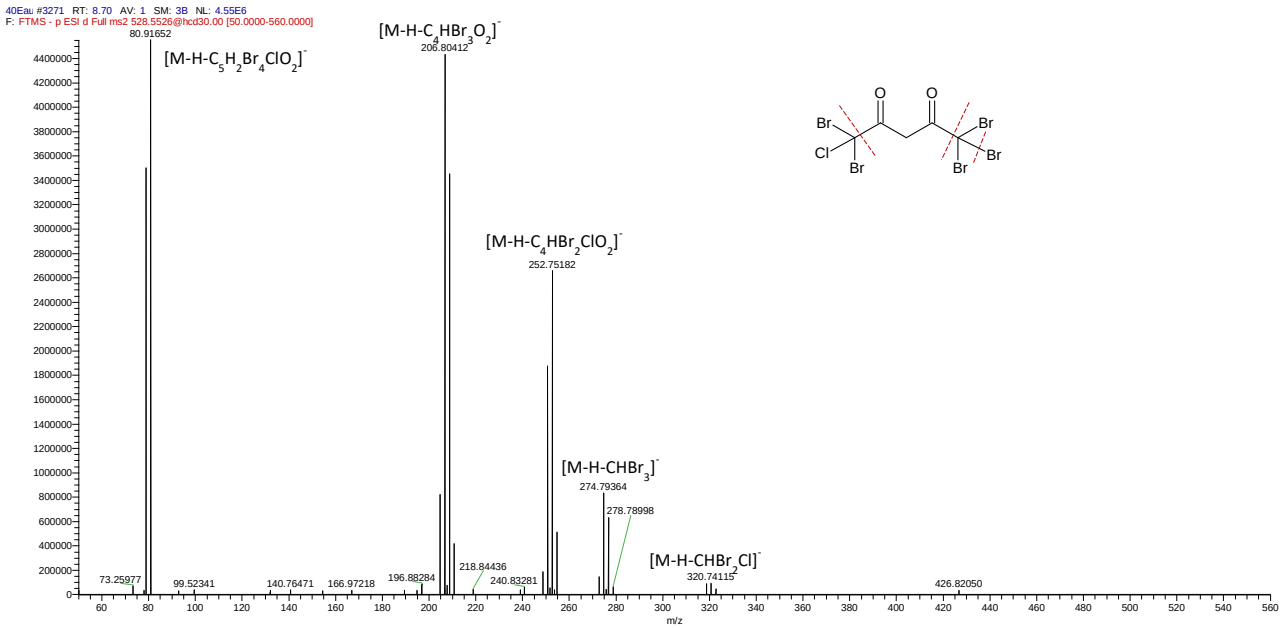

**Figure S6: ESI(−)-MS/MS spectrum of $C_5H_3Br_4ClO_2$ (compound 5) and the possible fragmentation pattern.**

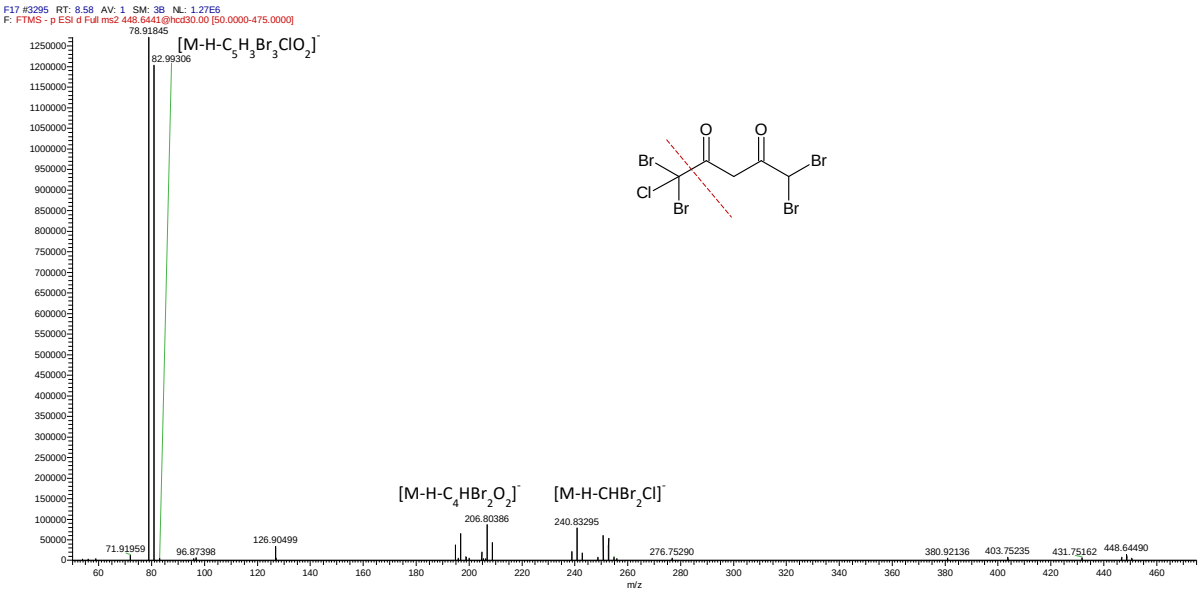


**Figure S7: ESI(−)-MS/MS spectrum of $C_4H_3Br_3O_3$ (compound 6) and the possible fragmentation pattern.**

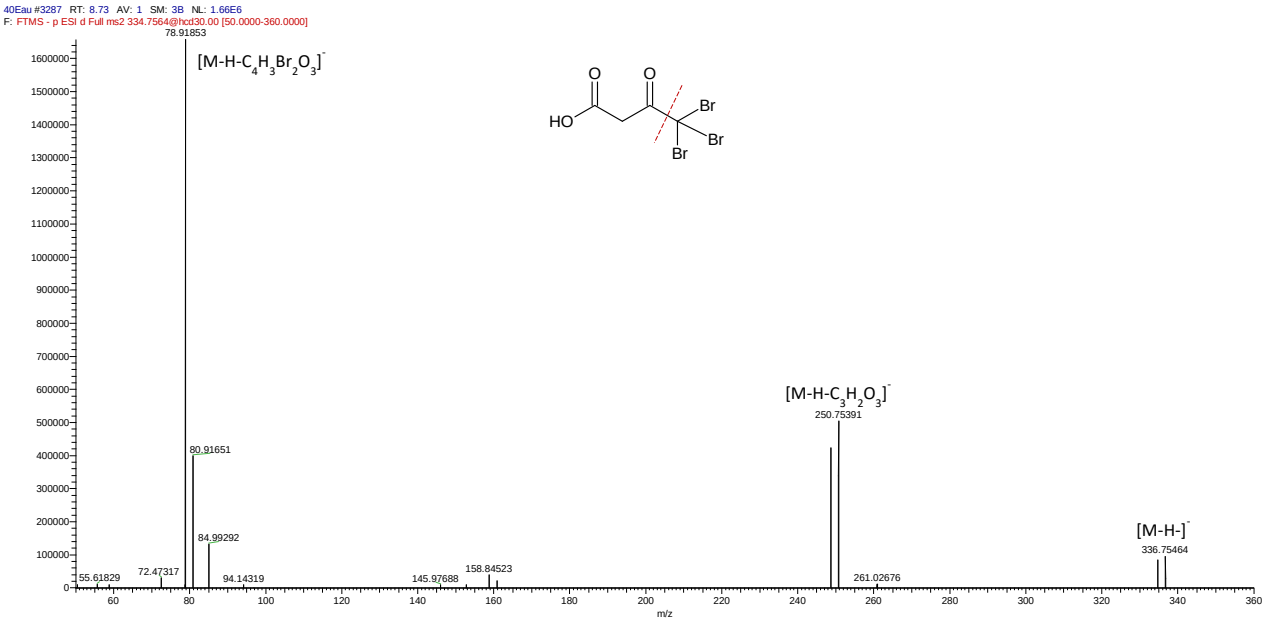

**Figure S8: ESI(−)-MS/MS spectrum of $C_5H_3Br_5O_2$ (compound 7) and the possible fragmentation pattern.**

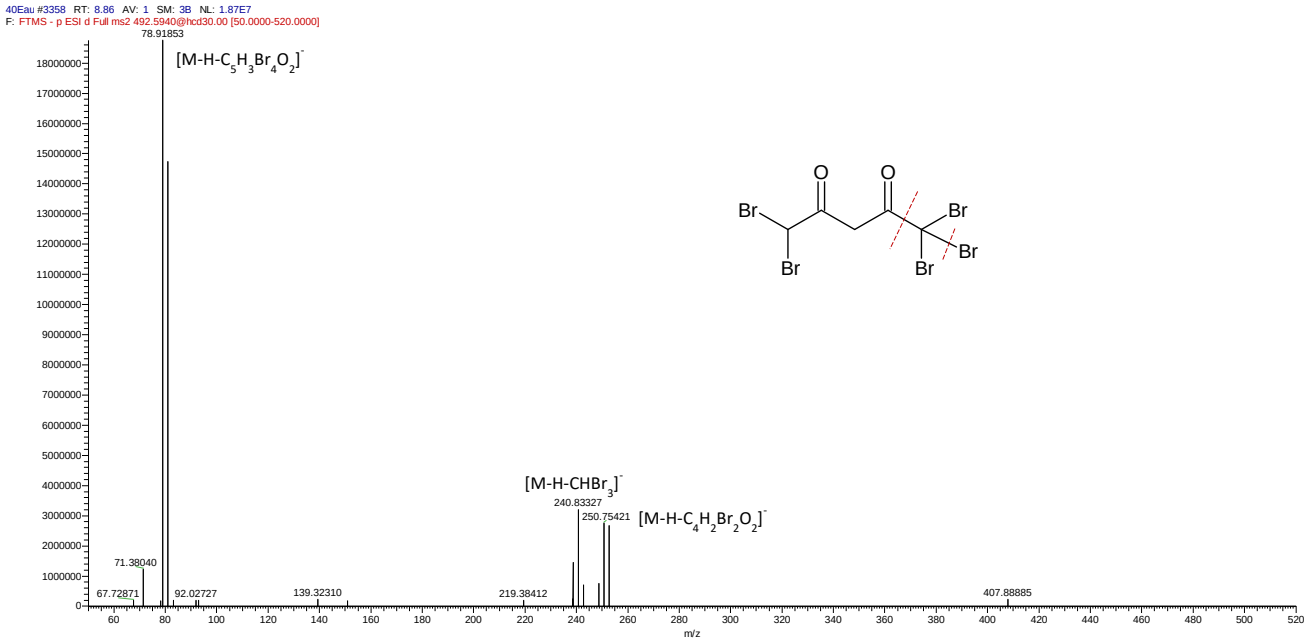

**Figure S9: Chromatogram of the most active fractions of the second fractionation (HPLC (Waters 1525) coupled to a UV detector (Waters 2487)) analysed by UHPLC-ESI(−)-HRMS/MS**

A. F9 (99±0.0 % of bacterial growth inhibition)

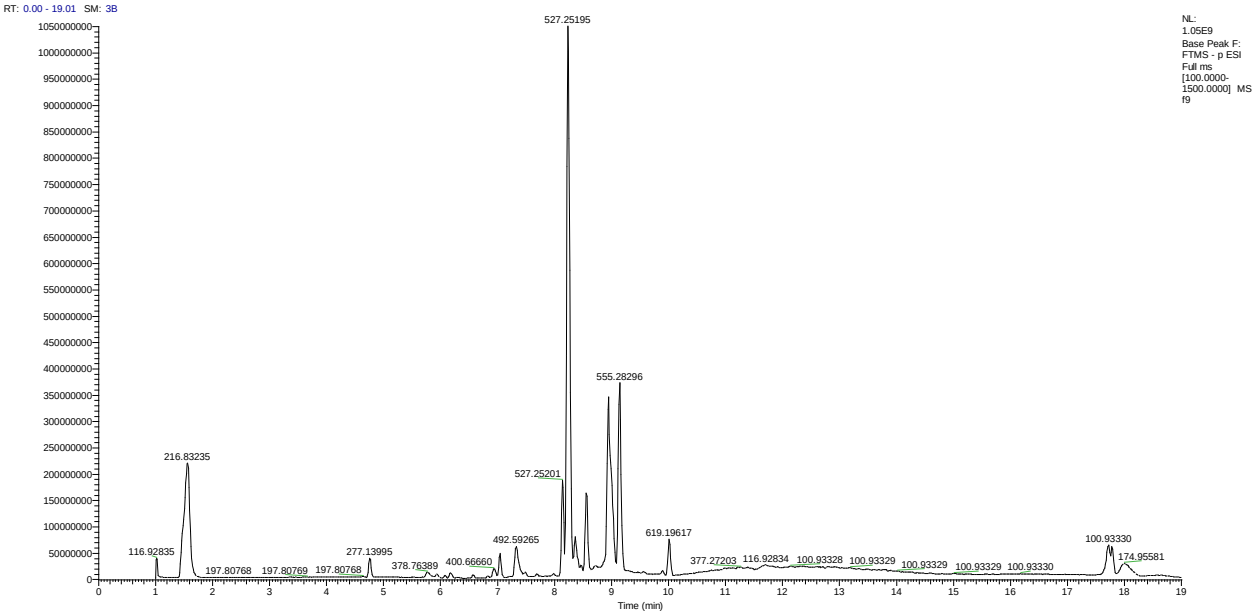


B. F10 (93.7±0.3 % of bacterial growth inhibition)

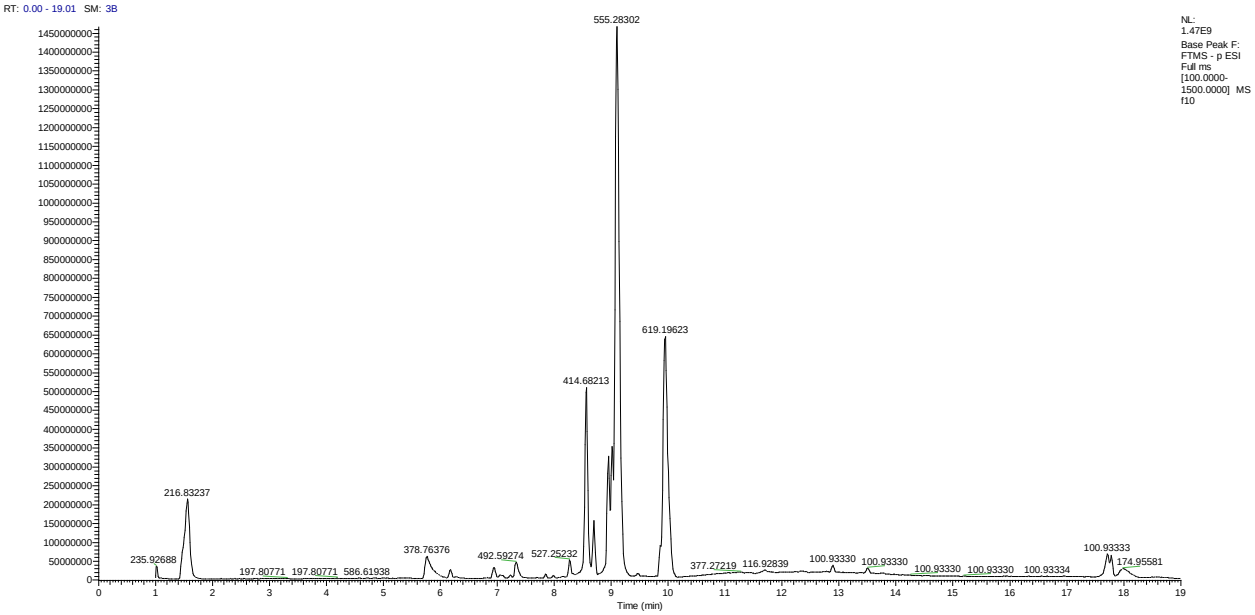

**Figure S10: EIC of ion with a *m/z* 572.5021 (most abundant isotopic mass) corresponding to a monoisotopic m/z of 566.5085 in active fractions, including 40 % $H_2O$-MeOH (A), 30 % $H_2O$-MeOH (B), F9 (C) and F10 (D).**

A. 40% $H_2O$-MeOH

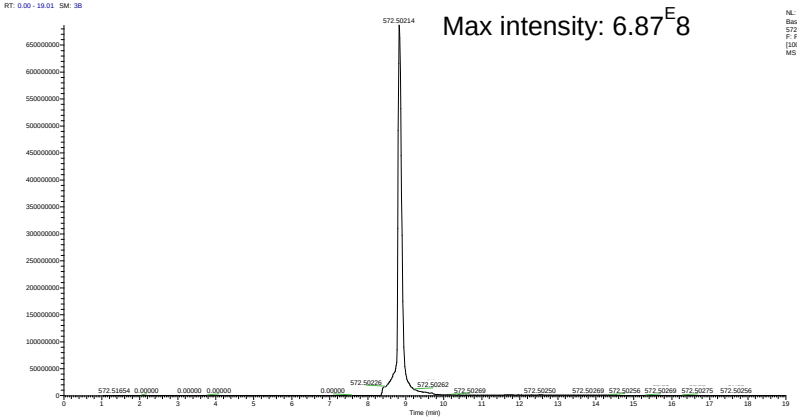


B. 30% $H_2O$-MeOH

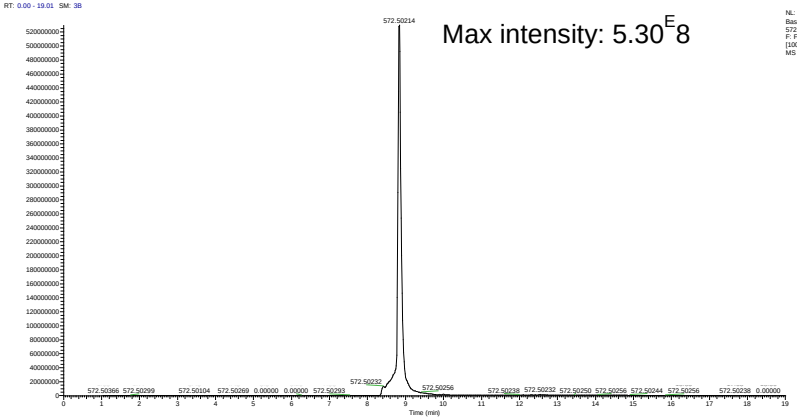


C. F9

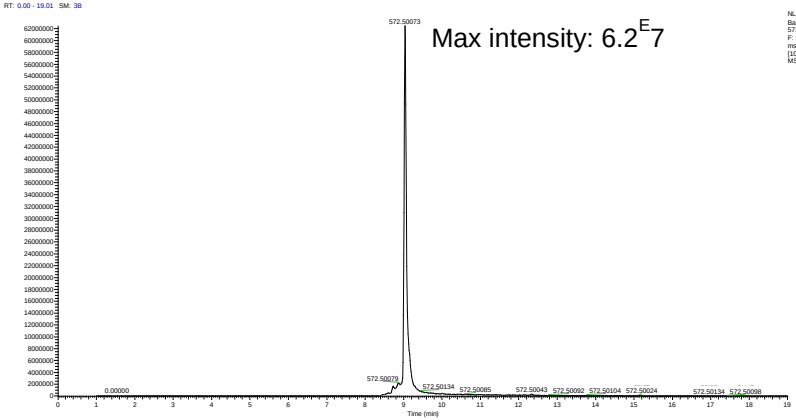


D. F10

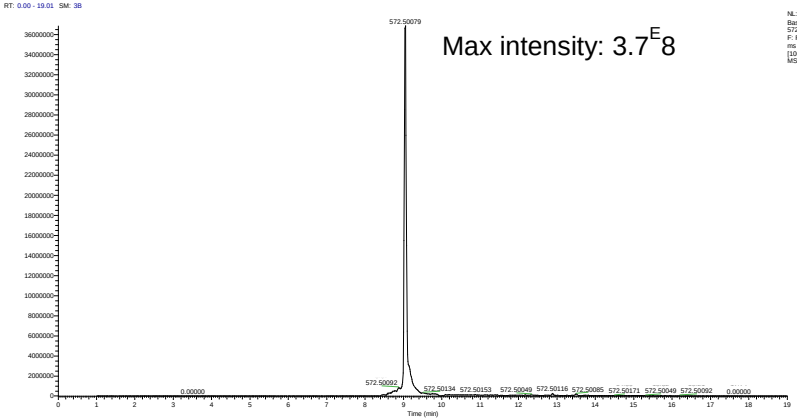

**Figure S11: Rarefaction curves of 16S rRNA gene sequences for the gametophyte with developed cystocarps (A), the gametophyte (B) and the tetrasporophyte (C) samples.**

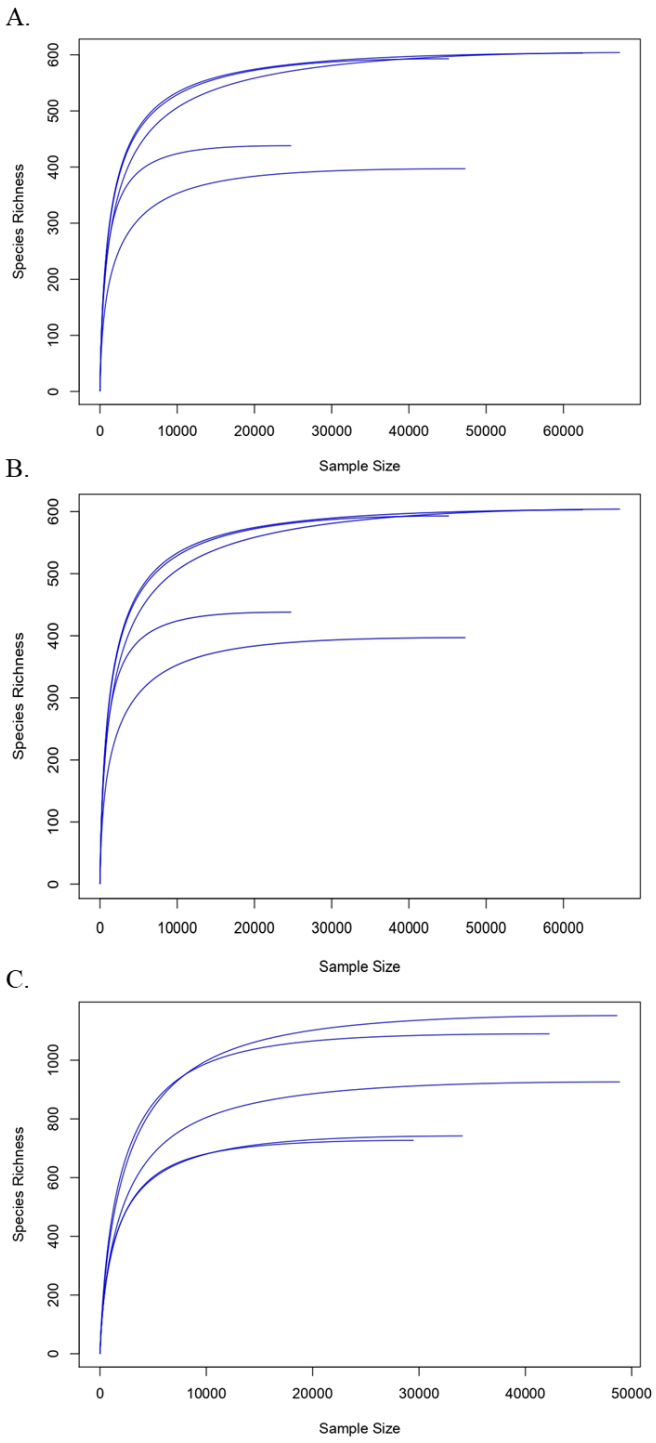

**Figure S12: Relative abundance of bacterial families associated with the three *A. armata* stages. Codes "C" represents samples of the gametophyte with developed cystocarps, "G" the gametophyte samples and "T" the tetrasporophyte samples.**

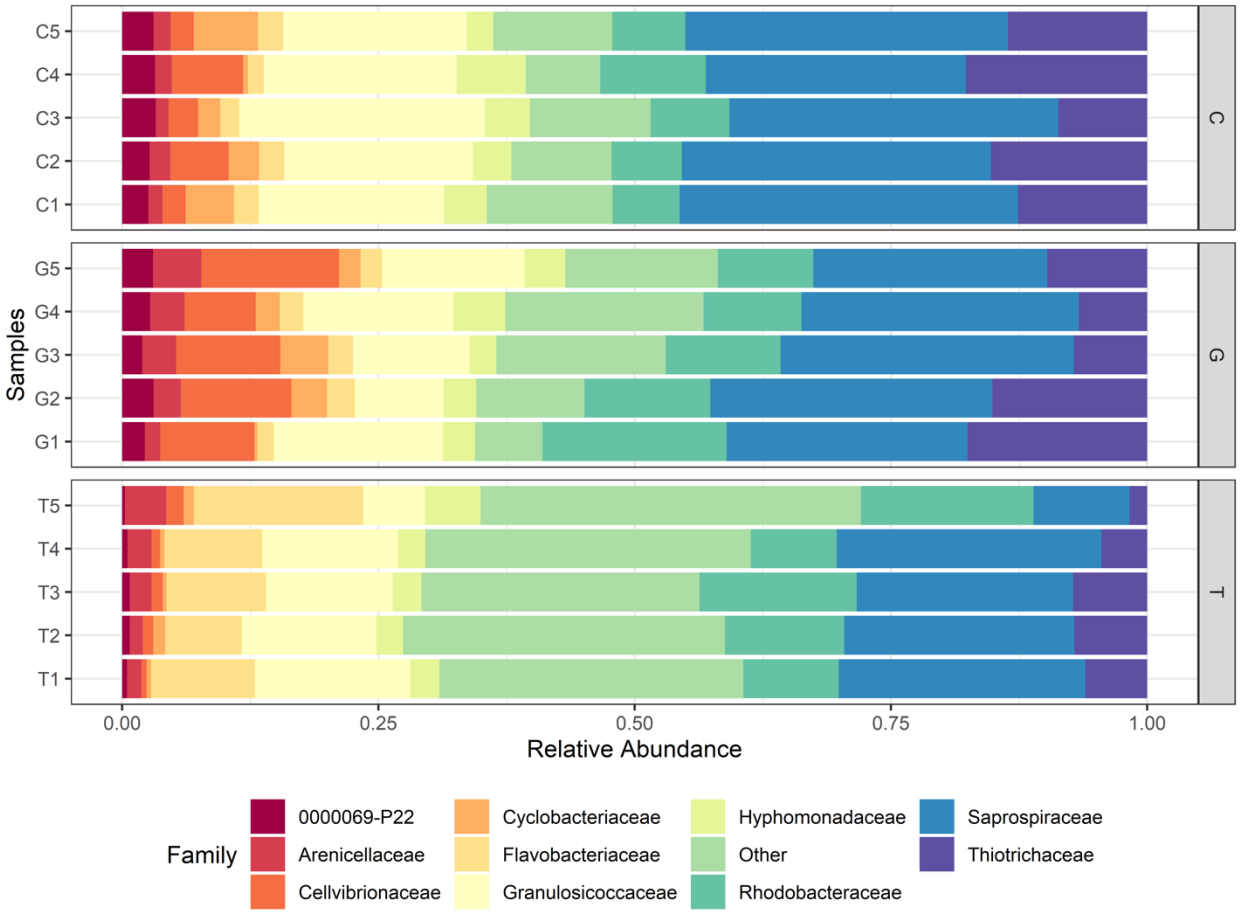

**Figure S13: KO pathways of the most predicted abundant functions associated with GC (A), G (B) and T (C).**

**Figure S14: Scores plot of the multiblock PLS-DA analysis (DIABLO) of *A. armata* gametophyte (G), with developed cystocarps (GC), and tetrasporophyte (T) phases.**

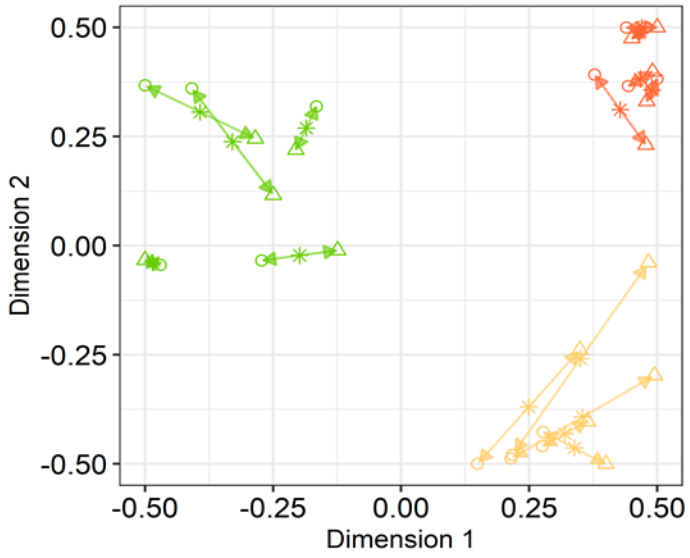


**Legend**

- Gametophyte (G)
- Gametophyte with developed cystocarps (GC)
- Tetrasporophyte (T)
- ○ Chemistry dataset
- △ Microbiota dataset
- ✳ Centroid

**Figure S15: Correlations between the first dimension (A) and the second dimension (B) of each dataset (Chem= Chemistry; Metabarc= Metabarcoding) for the two PLS models. Codes "C" represents samples of the gametophyte with developed cystocarps, "G" the gametophyte samples and "T" the tetrasporophyte samples.**

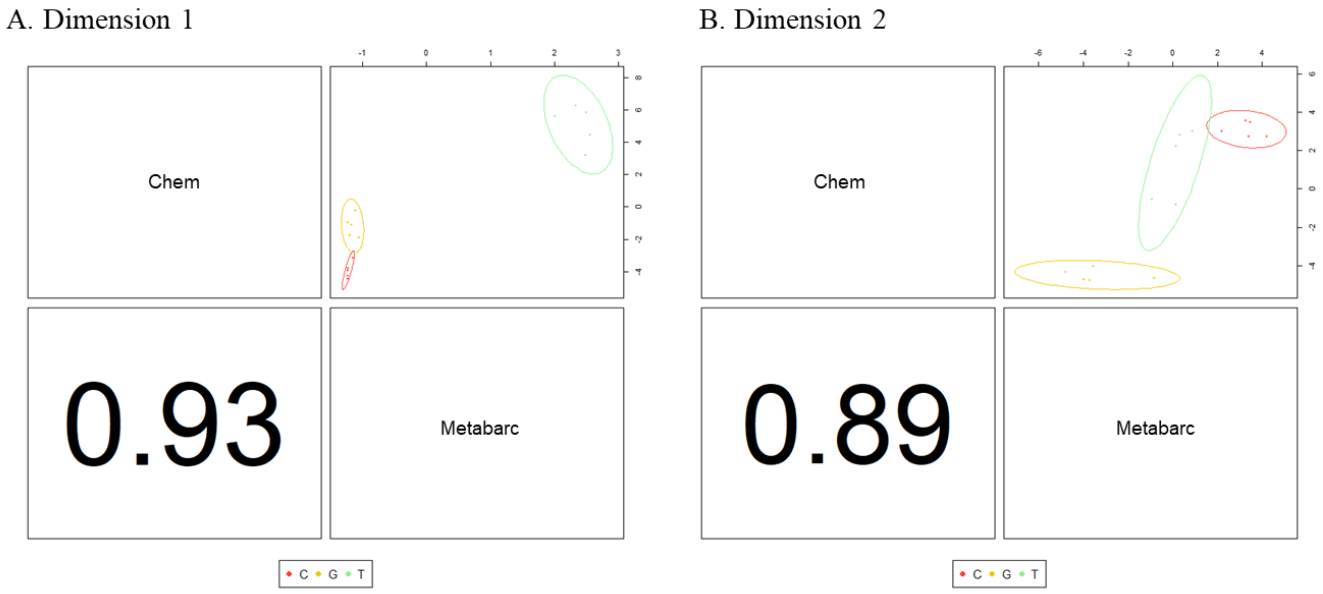

**Figure S16: Heatmap of significant ASV and metabolites of the three phases of *A. armata* ("GC" represents samples of the gametophyte with developed cystocarps, "G" the gametophyte samples and "T" the tetrasporophyte samples)**